Electronic Supplementary Material (ESI) for RSC Advances.


# Supporting Information

## Novel Decorated Aluminium (III) Phthalocyanine Complex with Appliance of MWCNTs on Electrodes: Electrochemical Nonenzymatic Oxidation and Reduction of Glucose and Hydrogen Peroxide

*Mounesh* [a,*], *P. Manikanta*[a], *K. R. Venugopala Reddy*[b], *C. C. Vidyasagar*[c], *Bhari Mallanna Nagaraja* [a,*]

[a,*]Centre for Nano and Material Science (CNMS), Jain (Deemed-to-be University), Jain Global Campus, Kanakapura, Bangalore, Karnataka, India – 562112

[b]Department of Studies and Research in Chemistry Vijayanagara Sri Krishnadevaraya University, Ballari – 583105, Karnataka, India

[c]Department of Studies and Research in Chemistry, Rani Channamma University, Belagavi – 591156, Karnataka, India

([*]Email: mounesh.m.nayak@gmail.com)

([*]Email: bm.nagaraja@jainuniversity.ac.in)

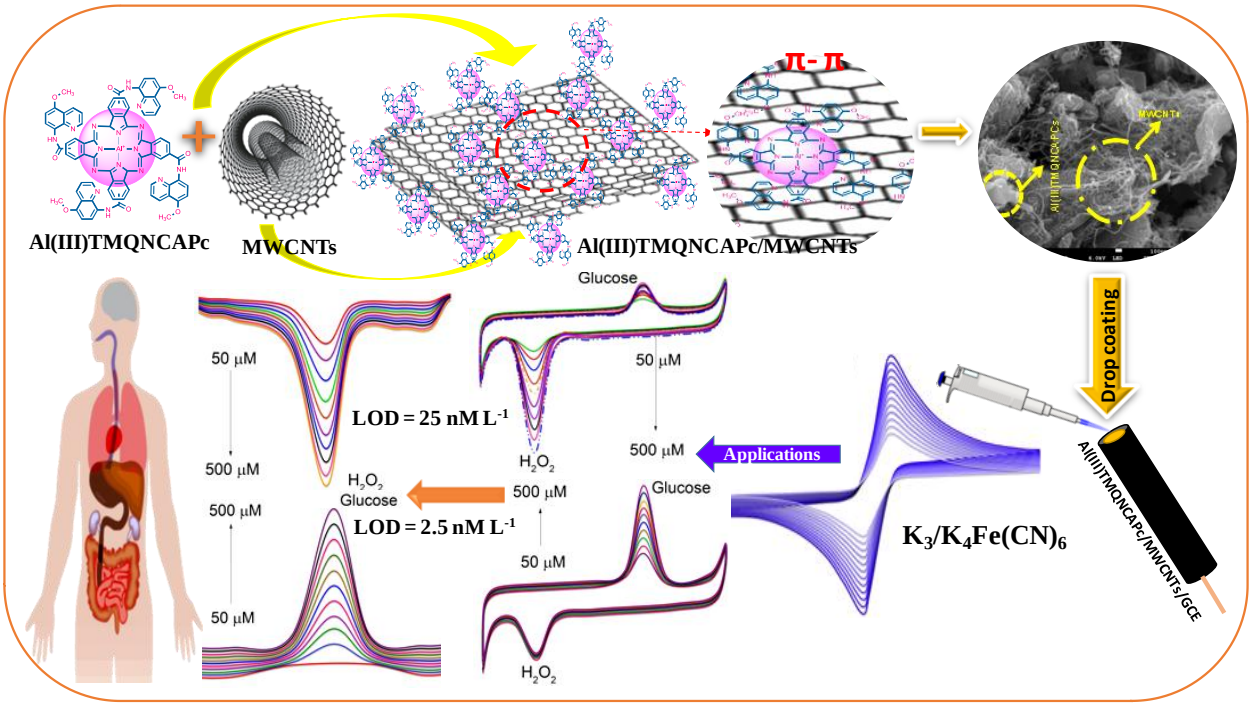
Al(III)TMQNCAPc
MWCNTs
Al(III)TMQNCAPc/MWCNTs
π- π
Drop coating
Al(III)TMQNCAPc/MWCNTs/GCE
Applications
K3/K4Fe(CN)6
LOD = 25 nM L-1
LOD = 2.5 nM L-1
Glucose
H2O2
50 μM
500 μM

## List of contents

## Experimental

### Reagents

2-Amino-5-Methoxyquinoline ($C_{10}H_{10}N_2O$), anhydrous potassium carbonate ($K_2CO_3$), dry DMF ($C_3H_7NO$), aluminium (III) chloride ($AlCl_3.6H_2O$), methanol ($CH_3OH$), ethanol ($C_2H_5OH$), acetone ($CH_3COCH_3$), ammonium chloride ($NH_4Cl$), *n*-hexane ($C_6H_{14}$), ammonium molybdate ($(NH_4)_2MoO_4$), trimellitic anhydride ($C_9H_4O_5$), sodium dihydrogen phosphate ($NaH_2PO_4.2H_2O$) and disodium hydrogen phosphate ($Na_2HPO_4.2H_2O$), N,N' Dicyclohexylcarbodiimide (DCC), glucose ($C_6H_{12}O_6$), hydrogen peroxide ($H_2O_2$), ascorbic acid (AA), dopamine (DA), uric acid (UA), L-cysteine (L-Cys), L-Alanine (L-Ala), L-Arginine (L-Arg), and dimethylsulfoxide (DMSO) were of analytical reagent (AR) grade reagents and procured from Sigma-Aldrich, India. The chemicals were used without any further purification and solution were prepared from double distilled water.

### Characterization method

The IR spectrum is recorded on a Perkin Elmer 1600 FT-IR spectrophotometer using KBr pellets. The thermo gravimetric analysis by STA6000 machine in the temperature range of 0 to 800 °C with the scan rate of 15 °C $min^{-1}$ under oxygen flow 30 $mL.min^{-1}$. Electronic spectra were recorded with a Perkin Elmer Lambda 25 spectrophotometer (UV-Vis). The Al(III)TMQNCAPc complex was studied by XRD using a (Model D8 Advance, Bruker) with a Cu- Kα1 X-ray radiation (λ = 0.15406 nm) diffractometer. The morphology and surface structure of Al(III)TMQNCAPc and Al(III)TMQNCAPc @MWCNTs were checked using the Sigma Field Emission Scanning Electron Microscope (Carl Zeiss Sigma VP FE-SEM). The CH analyzer instrument CHI6203E model with three electrode system composed of Glassy carbon electrode as a working electrode, platinum as counter electrode, silver/silver chloride (Ag/AgCl) electrode as reference electrode.

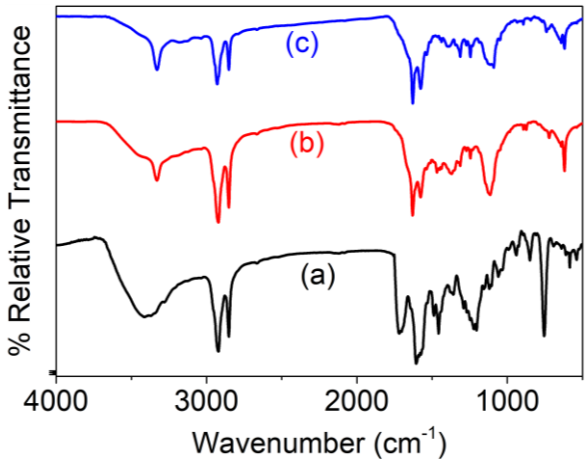


**Fig.S1:** FTIR spectra of (a) Al(III)TCAPc, (b) Al(III)TMQNCAPc, and (c) Al(III)TMQNCAPc@MWCNTs.

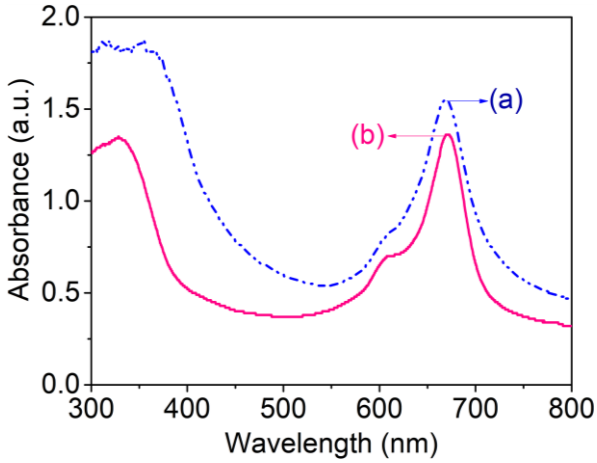


**Fig.S2:** UV-Vis spectra of inset (a) Al(III)TCAPc and (b) Al(III)TMQNCAPc.

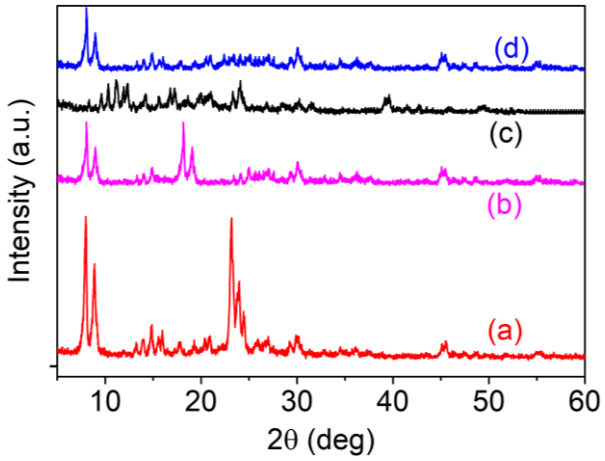


**Fig.S3:** Powder XRD analysis of (a) Al(III)TCAPc, (b) Al(III)TMQNCAPc, (c) MWCNTs and (d) Al(III)TMQNCAPc@MWCNTs.

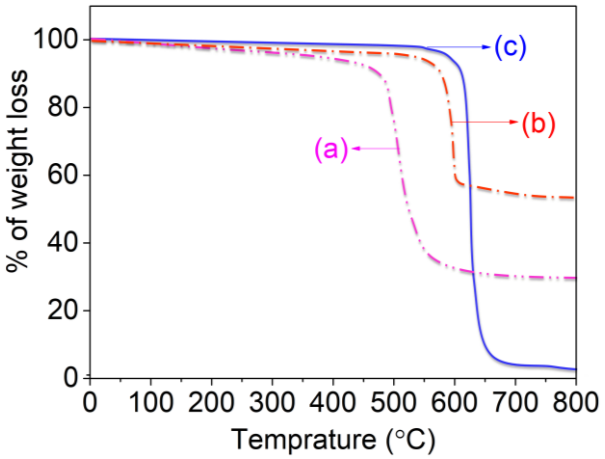


**Fig.S4:** Thermogravimetric analysis of (a) Al(III)TCAPc, (b) Al(III)TMQNCAPc, (c) Al(III)TMQNCAPc@MWCNTs.

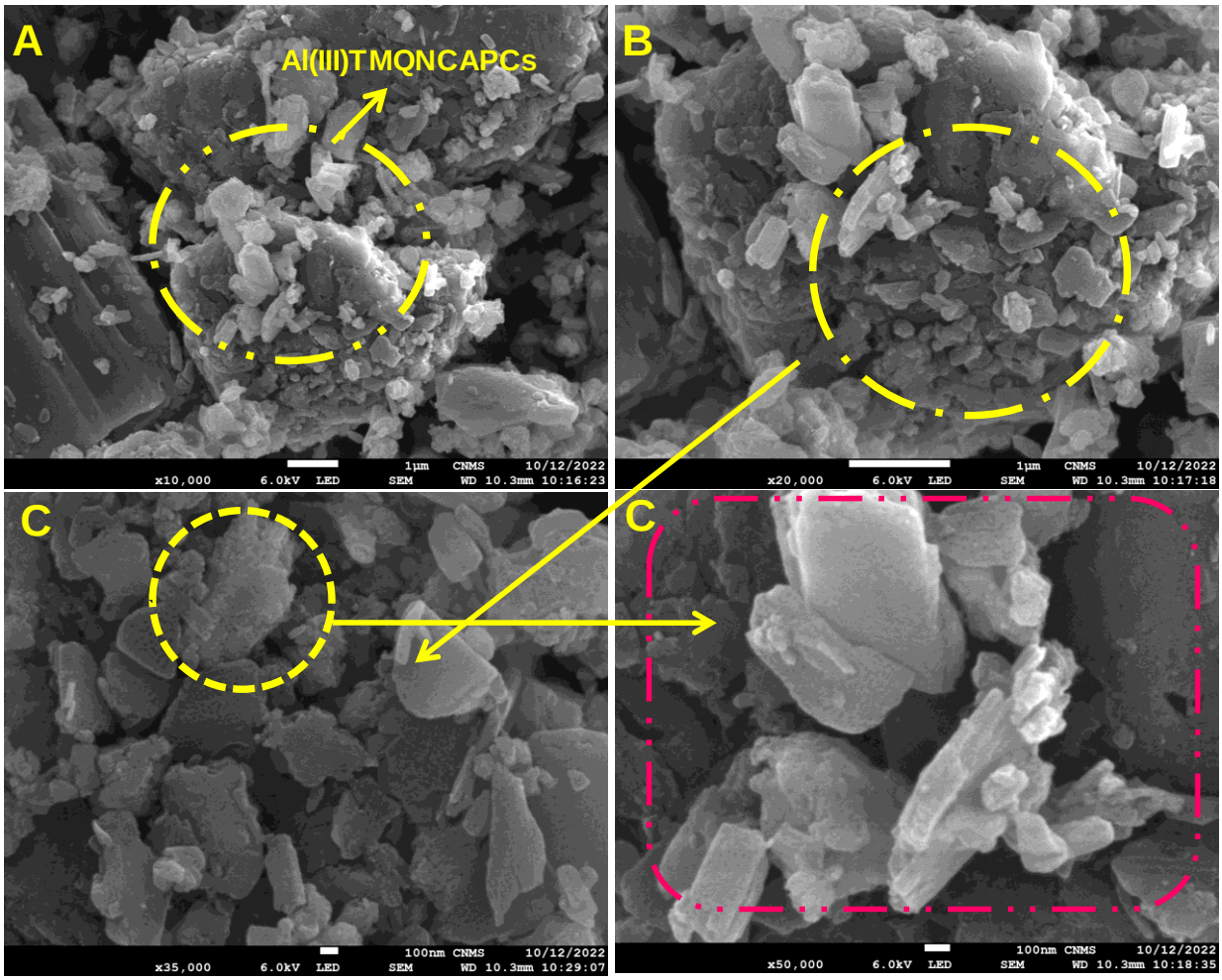


**Fig.S5:** FE-SEM analysis of (A-D) neat Al(III)TMQNCAPc catalyst.

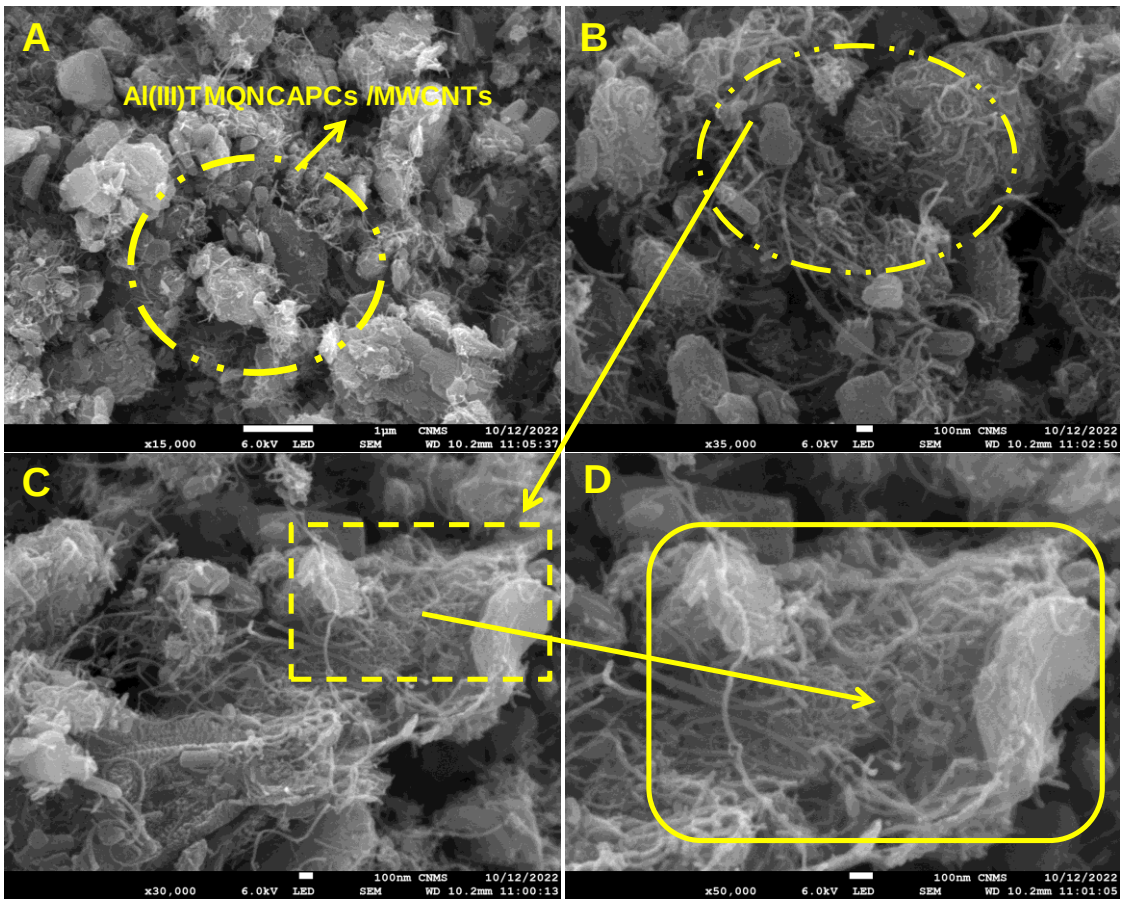


**Fig.S6:** FE-SEM analysis of (A-D) neat Al(III)TMQNCAPc@MWCNTs catalyst.

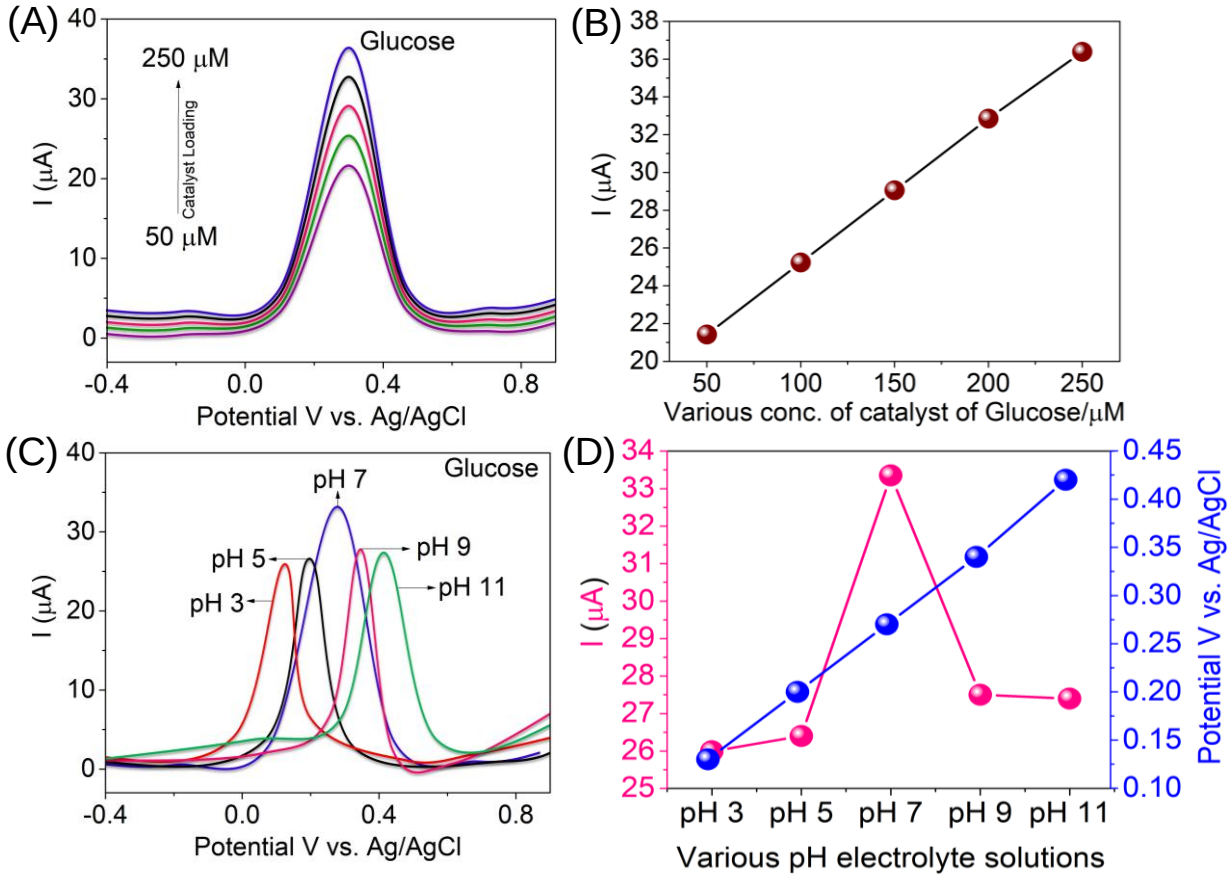


**Fig.S7:** Effect of catalyst loading and pH over glucose by AlTMQNCAPc@MWCNTs/GC electrode. (A) DPV response of glucose for different amount catalyst loading. (B) Dependence of current over the catalyst amount loaded. (B) DPV response of glucose at various pH. (D) Dependence of current and oxidation potential over pH of electrolyte**.**

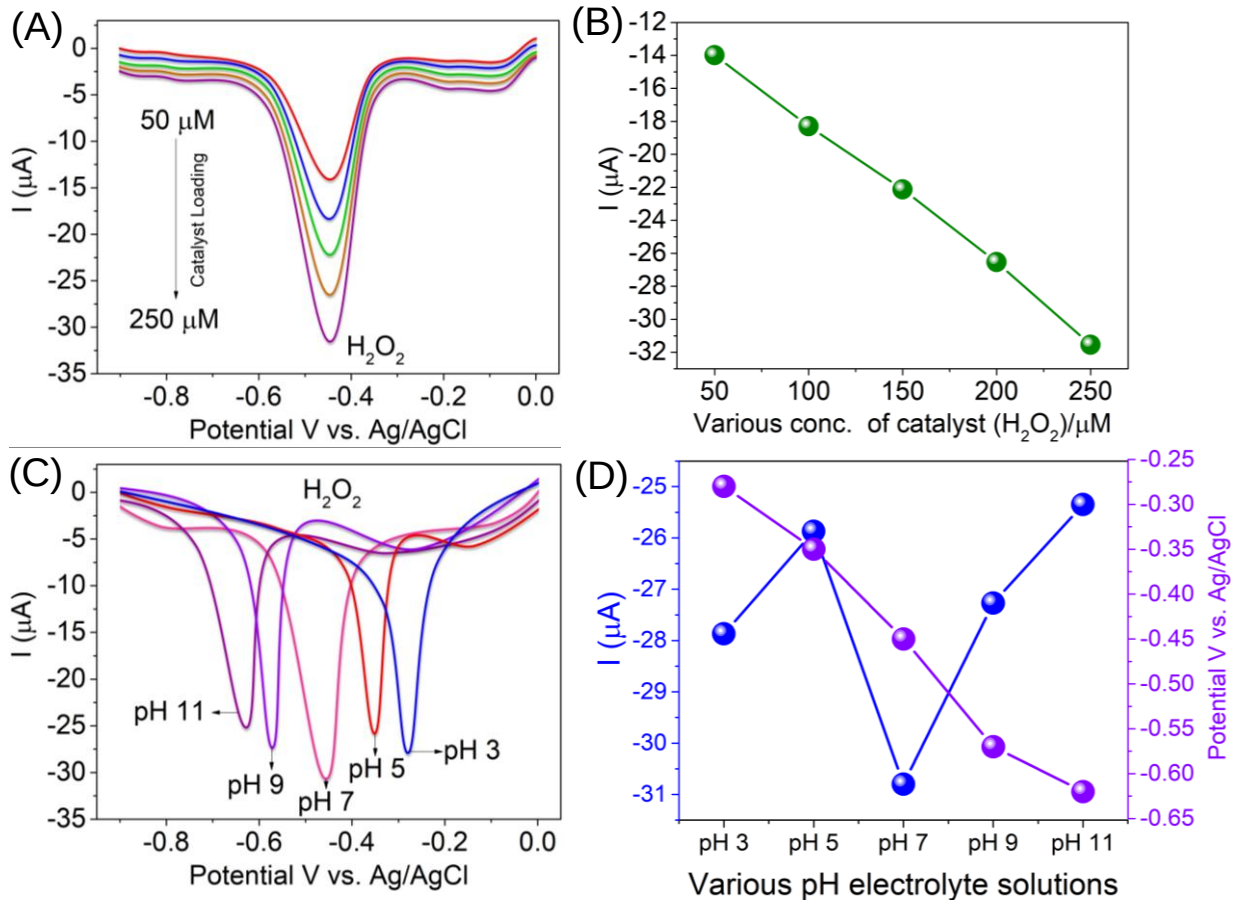


**Fig.S8:** Effect of catalyst loading and pH over $H_2O_2$ by AlTMQNCAPc@MWCNTs/GC electrode. (A) DPV response of $H_2O_2$ for different amount catalyst loading. (B) Dependence of current over the catalyst amount loaded. (B) DPV response of $H_2O_2$ at various pH. (D) Dependence of current and reduction potential over pH of electrolyte**.**

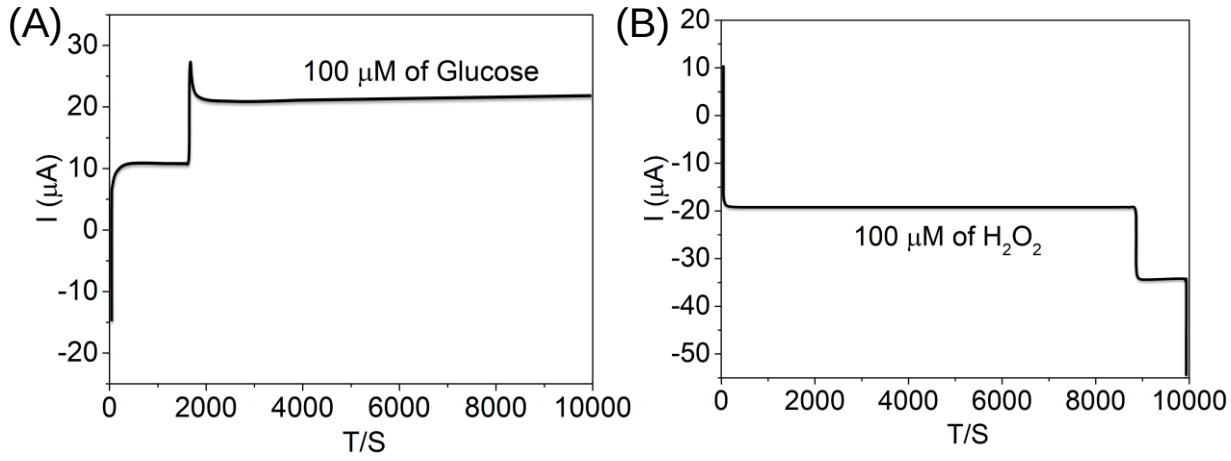


**Fig.S9:** (A) Operational stability of the AlTMQNCAPc@MWCNTs/GC electrode under continuous response at the optimized potential of +0.3 V in a stirred PBS (pH 7) containing 100 μM glucose. (B) Operational stability of the AlTMQNCAPc@MWCNTs/GC electrode under continuous response at the optimized potential of -0.45 V in a stirred PBS (pH 7) containing 100 μM $H_2O_2$.

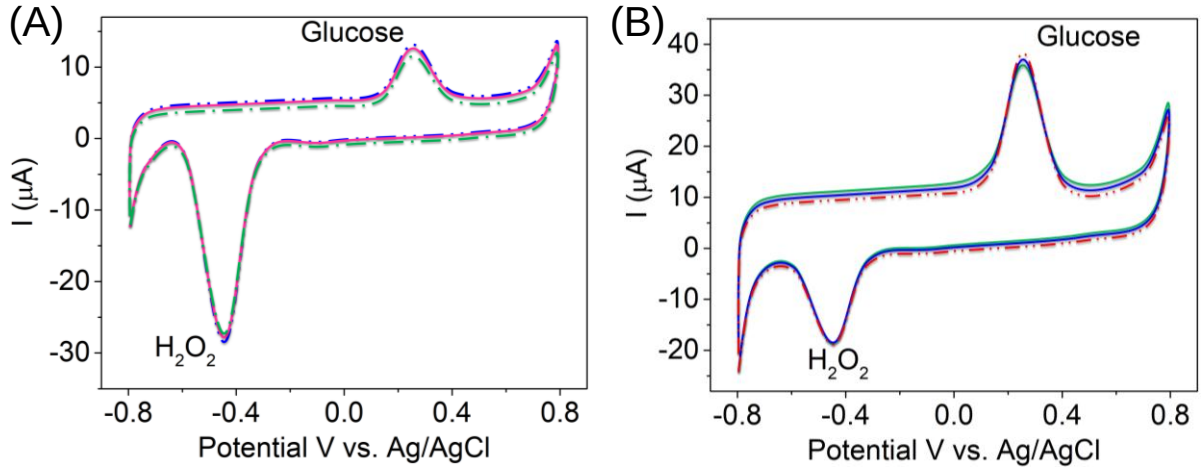


**Fig.S10:** (A) Ten successive CVs 100 μM of glucose in presence of $H_2O_2$. (B) Ten successive CVs 100 μM of $H_2O_2$ in presence of glucose by AlTMQNCAPc@MWCNTs/GC electrode in PBS (pH 7) solution at scan rate of 0.10 V $s^{-1}$.

**Table S1.** Comparison of the results for glucose oxidation and $H_2O_2$ reduction with the literature reports.

| Electrode Materials | LOD | Linear range | Sensitivity | Ref. |
|---|---|---|---|---|
| **Glucose** | | | | |
| CuO/MWCNTs | 0.2 µM $L^{-1}$ | Up to 1.2 mM $L^{-1}$ | 2596 µA $mM^{-1}$ $cm^{-2}$ | [1] |
| CuO-rGO | 0.1 µM $L^{-1}$ | 0.0004–12 mM $L^{-1}$ | 2221 µA $mM^{-1}$ $cm^{-2}$ | [2] |
| Au/LDH-CNTs-G | 1.00 µM $L^{-1}$ | 10 - 6100 µmol $L^{-1}$ | 1989 µA $mM^{-1}$ $cm^{-2}$ | [3] |
| AuNPs/G/MWCNTs/GCE | 4.8 µM $L^{-1}$ | 10 - 350 µmol $L^{-1}$ | 0.03 µA $µM^{-1}$ $cm^{-2}$ | [4] |
| Ag@ZIF-67@MWCNT/NF | 0.49 µM $L^{-1}$ | 33 - 400 µmol $L^{-1}$ | 13.014 µA $µM^{-1}$ $cm^{-2}$ | [5] |
| Ni3S2/CNT | 1.0 µM $L^{-1}$ | 0.03−0.5 mM $L^{-1}$ | 3345 µA $mM^{-1}$ $cm^{-2}$ | [6] |
| CNT-Ni | 2 µM $L^{-1}$ | 0.005−2 mM $L^{-1}$ | 1384.1 µA $mM^{-1}$ $cm^{-2}$ | [7] |
| CoPc/G/IL | 0.67 µM $L^{-1}$ | 0.01–1.3 mM $L^{-1}$ | - | [8] |
| CoPc–$(CoTPP)_4$ | 10 µM $L^{-1}$ | 2–11 mM $L^{-1}$ | 0.03 µA $mM^{-1}$ $cm^{-2}$ | [9] |
| PG/OPPyNF/CoPcTS | 0.1 µM $L^{-1}$ | 0.25–20 mM $L^{-1}$ | 5.69 µA $mM^{-1}$ $cm^{-2}$ | [10] |
| **AlTMQNCAPc@MWCNTs/GC electrode** | **2.5 nM $L^{-1}$**<br>**3.1 nM $L^{-1}$**<br>**10 nM $L^{-1}$** | **50 - 500 µmol $L^{-1}$**<br>**50 - 500 µmol $L^{-1}$**<br>**50 - 500 µmol $L^{-1}$** | **0.058 µA $µM^{-1}$ $cm^{-2}$**<br>**0.062 µA $µM^{-1}$ $cm^{-2}$**<br>**0.098 µA $µM^{-1}$ $cm^{-2}$** | **This work** |
| **Hydrogen Peroxide** | | | | |
| Fe3O4 – MWCNT ink | 0.5 mM $L^{-1}$ | 0.001 - 2 µmol $L^{-1}$ | 1040 µA $µM^{-1}$ $cm^{-2}$ | [11] |
| PtNPs-SeNPs-FTO | 7.1 µM $L^{-1}$ | 0.01–40 mmol $L^{-1}$ | 7.3 µA $µM^{-1}$ $cm^{-2}$ | [12] |
| LSDC-GA | 1.2 µM $L^{-1}$ | 0.012-2.7 µmol $L^{-1}$ | 2.12 µA $µM^{-1}$ $cm^{-2}$ | [13] |
| $Sm_2CuO_4$/GCE | 0.41 µM $L^{-1}$ | 1.24~35.44 µmol $L^{-1}$ | 9.3 mA $µM^{-1}$ $cm^{-2}$ | [14] |
| $ZnCrCoO_4$/NCNTs | 1.0 µM $L^{-1}$ | 1~7.33 µmol $L^{-1}$ | - | [15] |
| Pd/$ZnFe_2O_4$/rGO/GCE | 2.12 mM $L^{-1}$ | 25~10.2 µmol $L^{-1}$ | 621.64 µA $µM^{-1}$ $cm^{-2}$ | [16] |
| Ag/$MnO_2$ /GO/GCE | 0.7 µM $L^{-1}$ | 3~7 µmol $L^{-1}$ | 105.4 µA $µM^{-1}$ $cm^{-2}$ | [17] |
| $ZnCrCoO_4$/NCNTs | 1.0 µM $L^{-1}$ | 1~7.33 µmol $L^{-1}$ | - | [18] |
| Pt/$Fe_3O_4$/rGO/GCE | 1.58 µM $L^{-1}$ | 100~2.4 µmol $L^{-1}$ | 6.875 µA $mM^{-1}$ $cm^{-2}$ | [19] |
| Ag/$MnO_2$/MWCNTs/GCE | 1.7 µM $L^{-1}$ | 5~10.4 µmol $L^{-1}$ | 82.5 µA $mM^{-1}$ $cm^{-2}$ | [20] |
| **AlTMQNCAPc@MWCNTs/GC electrode** | **25 nM $L^{-1}$**<br>**18 nM $L^{-1}$**<br>**20 nM $L^{-1}$** | **50 - 500 µmol $L^{-1}$**<br>**50 - 500 µmol $L^{-1}$**<br>**50 - 500 µmol $L^{-1}$** | **0.072 µA $µM^{-1}$ $cm^{-2}$**<br>**0.066 µA $µM^{-1}$ $cm^{-2}$**<br>**0.053 µA $µM^{-1}$ $cm^{-2}$** | **This work** |

**Table S2.** Analytical data obtained for the commercial 3% $H_2O_2$ in clinic product samples.

| Samples | Theoretical valve ($\mu M\ L^{-1}$) | Detected ($\mu M\ L^{-1}$) | Spiking ($\mu M\ L^{-1}$) | Recovery (n =3, %) |
|---|---|---|---|---|
| Sample 1 | 50 | 54 | 25 | 92.59 % |
| Sample 2 | 100 | 101 | 50 | 99.00 % |
| Sample 3 | 150 | 151 | 75 | 101.33 % |

**Table S3.** Determination of glucose in the human urine samples.

| Samples | Theoretical valve ($\mu M\ L^{-1}$) | Detected ($\mu M\ L^{-1}$) | Spiking ($\mu M\ L^{-1}$) | Recovery (n =3, %) |
|---|---|---|---|---|
| Sample 1 | 100 | 104 | 55 | 96.15 % |
| Sample 2 | 200 | 201 | 100 | 99.50 % |
| Sample 3 | 300 | 300.34 | 150 | 102.33 % |

## References


1. Jiang, L.-.C.; Zhang, W.-.D. A highly sensitive nonenzymatic glucose sensor based on CuO nanoparticles-modified carbon nanotube electrode. *Biosens. Bioelectron.* **2010**, *25*, 1402–1407.
2. Wang, X.; Liu, E.; Zhang, X. Non-enzymatic glucose biosensor based on copper oxide-reduced graphene oxide nanocomposites synthesized from water-iso- propanol solution. *Electrochim. Acta.* **2014**, *130,* 253–260.
3. Kang, L.Q.; He, D.P.; Bie, L.L.; Jiang, P. Nanoporous cobalt oxide nanowires for non-enzymatic electrochemical glucose detection. *Sensor. Actuator. B Chem.* **2015**, *220,* 888-894.
4. Y. Yu. Direct electron transfer of glucose oxidase and biosensing for glucose based on PDDA-capped gold nanoparticle modifed graphene/multi-walled carbon nanotubes electrode. *Biosens. Bioelectron.* **2014,** *52,* 147–152.
5. Elizbit.; Liaqat, U.; Hussain, Z.; Baig, M. M.; Khan, M. A.; Arif, D. Preparation of porous ZIF‐67 network interconnected by MWCNTs and decorated with Ag nanoparticles for improved non‐enzymatic electrochemical glucose sensing. *Journal of the Korean Ceramic Society*. **2021**, *58,* 598–605
6. Lin, T. W.; Liu, C. J.; Dai, C. S. Ni3S2/carbon nanotubes nanocomposite as electrode material for hydrogen evolution reaction in alkaline electrolyte and enzyme-free glucose detection. *Appl. Catal., B.* **2014,** 213−220.
7. Choi, T.; Kim, S. H.; Lee, C. W.; Kim, H.; Choi, S.-K.; Kim, S.-H.; Kim, E.; Park, J.; Kim, H. Synthesis of carbon nanotube−nickel nanocomposites using atomic layer deposition for high-performance non-enzymatic glucose sensing. *Biosens. Bioelectron.* **2015,** *63,* 325−330.
8. Chaiyo, S.; Mehmeti, E.; Siangproh, W.; Hoang, T.L.; Nguyen, H.P.; Chailapakul, O.; Kalcher, K. Non-enzymatic electrochemical detection of glucose with a disposable paper-based sensor using a cobalt phthalocyanine–ionic liquid–graphene composite. *Biosens. Bioelectron.* **2018**, *102,* 113–120.
9. Ozoemena, K. I.; Nyokong, T. Novel amperometric glucose biosensor based on an ether-linked cobalt (II) phthalocyanine–cobalt(II) tetraphenylporphyrin pentamer as a redox mediator. *Electrochim Acta.* **2006**, *51*, 5131–5136.

10. Levent, O.; Yucel, S.; Turk, H. Non-enzymatic glucose biosensor based on overoxidized polypyrrole nanofiber electrode modified with cobalt (II) phthalocyanine tetra sulfonate. *Biosens Bioelectron*. **2008**, *24*, 512–517.
11. Garate, O.; Veiga, L. S.; Tancredi, P.; Medrano, A. V.; Monsalve, L. N.; Ybarra, G. High-performance non-enzymatic hydrogen peroxide electrochemical sensor prepared with a magnetite-loaded carbon nanotube waterborne ink. *Journal of Electroanalytical Chemistry*. **2022**, *915*, 116372.
12. Dumore, N. S.; Mukhopadhyay, M. Development of novel electrochemical sensor based on PtNPs-SeNPs-FTO nanocomposites via electrochemical deposition for detection of hydrogen peroxide. *Journal of Environmental Chemical Engineering.* **2022**, *10*, 107058.
13. Dong, S.; Guo, L.; Chen, Y.; Zhang, Z.; Yang, Z.; Xiang, M. Three-dimensional loofah sponge derived amorphous carbon-graphene aerogel via one-pot synthesis for high-performance electrochemical sensor for hydrogen peroxide and dopamine. *Journal of Electroanalytical Chemistry.* **2022**, *911*, 116236.
14. Wang, X-T.; Li, B.; Kong, D-R.; Zhang, Z-Y.; Zhang, X-F.; Deng, Z-P.; Huo, L-H.; Gao, S. *T*- and *T′*-type layered perovskite Ln2CuO4 nanocrystals for enhanced sensing detection of hydrogen peroxide. *Journal of Alloys and Compounds.* **2022**, *911*, 165037.
15. Ning, L.; Liu, Y.; Ma, J.; Fan, X.; Zhang, G.; Zhang, F.; Peng, W.; Li, Y. Synthesis of Palladium, $ZnFe_2O_4$ Functionalized Reduced Graphene Oxide Nanocomposites as $H_2O_2$ Detector. *Ind. Eng. Chem. Res.* **2017**, *56*, 4327-4333.
16. Liu, W.; Zhou, Z.; Yin, L.; Zhu, Y.; Zhao, J.; Zhu, B.; Zheng, L.; Jin, Q.; Wang, L. A novel self-powered bioelectrochemical sensor based on $CoMn_2O_4$ nanoparticle modified cathode for sensitive and rapid detection of hydrogen peroxide. *Sensors Actuators B: Chem.* **2018**, *271*, 247-255.
17. Zhang, J.; Rao, D.; Zheng, J. Synthesis of Ag Nanoparticle Doped $MnO_2$/GO Nanocomposites at a Gas/Liquid Interface and its Application in $H_2O_2$ Detection. *Electroanalysis.* **2016**, *28*, 588-595.
18. Wu, H.; Xiao, K.; Ouyang, T.; Wang, Z.; Chen, Y.; Li, N.; Liu, Z.Q. Co-Cr mixed spinel oxide nanodots anchored on nitrogen-doped carbon nanotubes as catalytic electrode for hydrogen peroxide sensing. *J. Colloid Interface Sci.* **2021**, *585*, 605-613.

19. Zhao, X.; Li, Z.; Chen, C.; Wu, Y.; Zhu, Z.; Zhao, H.; Lan, M. A Novel Biomimetic Hydrogen Peroxide Biosensor Based on Pt Flowers-decorated $Fe_3O_4$/Graphene Nanocomposite. *Electroanalysis.* **2017**, *29*, 1518-1523.
20. Han, Y.; Zheng, J.; Dong, S. A novel nonenzymatic hydrogen peroxide sensor based on Ag–$MnO_2$–MWCNTs nanocomposites. *Electrochim. Acta.* **2013**, *90*, 35-43.